



## Molecular flexibility and structural instabilities in crystalline L-methionine

Jennifer Fischer<sup>a,b,1</sup>, José A. Lima<sup>c</sup>, Paulo T.C. Freire<sup>c</sup>, Francisco E.A. Melo<sup>c</sup>, Remco W.A. Havenith<sup>d</sup>, Josué Mendes Filho<sup>c</sup>, Ria Broer<sup>d</sup>, Juergen Eckert<sup>e,f,\*</sup>, Heloisa N. Bordallo<sup>b,g</sup>

<sup>a</sup> Institute of Physics and Center for Interdisciplinary Nanostructure Science and Technology (CINSaT), University of Kassel, Heinrich-Plett-Str. 40, 34132 Kassel, Germany

<sup>b</sup> Helmholtz Zentrum Berlin für Materialien und Energie, Hahn Meitner Platz 1, 14109 Berlin, Germany

<sup>c</sup> Departamento de Física, Universidade Federal do Ceará, CP 6030, CEP 60455-760 Fortaleza, CE, Brazil

<sup>d</sup> Theoretical Chemistry, Zernike Institute for Advanced Materials, University of Groningen, Nijenborgh 4, 9747 AG Groningen, The Netherlands

<sup>e</sup> Department of Chemistry, University of South Florida, 4202 E. Fowler Ave., Tampa, FL 33620, USA

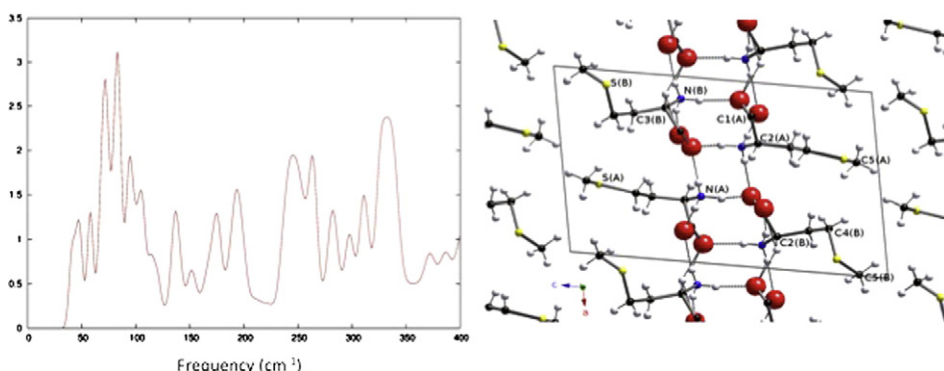
<sup>f</sup> Lujan Center, LANSCE, MS H05, Los Alamos National Laboratory, Los Alamos, NM 87545, USA

<sup>g</sup> Niels Bohr Institute, University of Copenhagen, Universitetsparken 5, 2100 Copenhagen, Denmark

### HIGHLIGHTS

- L-Methionine has a dynamically disordered structure at room temperature connected to the flexibility of the thiol-ether group.
- It undergoes a structural phase transition at body temperature.
- The room temperature structure is only recovered after 15min of relaxation time upon warming.
- Reorientational dynamics of the methyl group appear as precursor to conformational changes in L-methionine.

### GRAPHICAL ABSTRACT



### ARTICLE INFO

#### Article history:

Received 9 May 2013

Received in revised form 14 June 2013

Accepted 14 June 2013

Available online 28 June 2013

#### Keywords:

Amino acid  
Flexibility  
Structure  
Dynamics  
Spectroscopy  
Computation

### ABSTRACT

We have investigated the dynamics in polycrystalline samples of L-methionine related to the structural transition at about 307 K by incoherent inelastic and quasielastic neutron scattering, X-ray powder diffraction as well as ab-initio calculations. L-Methionine is a sulfur amino acid which can be considered a derivative of alanine with the alanine R-group CH<sub>3</sub> exchanged by –CH<sub>2</sub>S–(CH<sub>2</sub>)<sub>2</sub>. Using X-ray powder diffraction we have observed at ~190 K an anomalous drop of the c-lattice parameter and an abrupt change of the β-monoclinic angle that could be correlated to the anomalies observed in previous specific heat measurements. Distinct changes in the quasielastic region of the neutron spectra are interpreted as being due to the onset and slowing-down of reorientational motions of the CH<sub>3</sub>–S group, are clearly distinguished above 130 K in crystalline L-methionine. Large-amplitude motions observed at low frequencies are also activated above 275 K, while other well-defined vibrations are damped. The ensemble of our results suggests that the crystalline structure of L-methionine is dynamically highly disordered above 275 K, and such disorder can be linked to the flexibility of the molecular thiol-ether group.

© 2013 Elsevier B.V. All rights reserved.

\* Corresponding author at: Department of Chemistry, University of South Florida, 4202 E. Fowler Ave., Tampa, FL 33620, USA.

E-mail addresses: [juergen@usf.edu](mailto:juergen@usf.edu) (J. Eckert), [bordallo@nbi.ku.dk](mailto:bordallo@nbi.ku.dk) (H.N. Bordallo).

<sup>1</sup> JF recent address: Forschungszentrum Jülich, Institut of Complex Systems, Marie Gökking, ICS-3, 52425 Jülich, Germany.

## 1. Introduction

Amino acids are small biomolecules with an average molecular weight of about 135 Da and are the principal building blocks of proteins and enzymes. The structure of a protein determines its function, and it is determined by the amino acid sequence and the H-bond network built up by the amino acid side chains. The amino acid residues play an important role in substrate binding particularly in the case enzymes. Amino acids naturally exist in a zwitterionic state where the carboxylic acid moiety donates a hydrogen to the basic amino group. L-Methionine ( $\text{HO}_2\text{CCH}(\text{NH}_2)\text{CH}_2\text{CH}_2\text{SCH}_3$ , hereafter L-MET) is one of only two sulfur containing amino acids with an unbranched and highly hydrophobic side chain [1,2]. MET is essential in the initiation of protein synthesis as it is encoded in the start codon [3,4]. Most MET residues are buried inside the proteins because of their hydrophobic side chain, while other residues on the protein surface can be oxidized to sulfoxides. These oxidation effects have been associated with the development and progression of neurodegenerative diseases associated with aging such as Alzheimer's and Parkinson's [5]. It is also now widely accepted that MET residues constitute an important antioxidant defense by acting as “molecular bodyguards” [6,7]. Finally, it is worth noting that MET side chains in proteins have been shown to possess unique structural properties, which result in a malleable non-polar surface that can easily adapt to a variety of other peptides [8].

Structural studies in crystalline samples have been reported by three groups [9–11] all of which found that L-MET crystallizes in the monoclinic  $P2_1$  space group with four molecules in the unit cell ( $Z = 4$ ) in a double layer structure consisting of hydrophilic and hydrophobic layers. The hydrophilic layers are linked together with H-bonds between the head groups  $\text{NH}_3^+$  and  $\text{CO}_2^-$ , while the hydrophobic layers are held together by van-der-Waals forces between the methyl groups (Fig. 1). The single crystal structures reported in [10] and [11] are very similar with lattice-parameters  $a = 9.498(5)\text{\AA}$ ,  $b = 5.189(5)\text{\AA}$ ,  $c = 15.318(5)\text{\AA}$ , and  $\beta = 97.69(1)^\circ$  at 300 K and  $a = 9.493(2)\text{\AA}$ ,  $b = 5.201(2)\text{\AA}$ ,  $c = 14.831(3)\text{\AA}$ , and  $\beta = 99.84(2)^\circ$  at 120 K, respectively. However, the lattice parameters of polycrystalline samples at room temperature were reported [9] to differ appreciably with  $a = 15.49\text{\AA}$ ,  $b = 3.84\text{\AA}$ ,  $c = 14.11\text{\AA}$  and  $\beta = 103.9^\circ$  albeit with the same symmetry. All of the structural investigations agree on the existence of two crystallographically distinct molecules in the unit cell which differ mainly in the side-chain torsion-angles. Here it is important to realize that the structural plasticity (or flexibility) of the MET side chain is likely to arise from the unusual properties of the  $[\text{C}^3-\text{C}^4-\text{S}-\text{C}^5]$  torsional unit, which is virtually flat, as was pointed out by Gellman [2]. Indeed, in our recent report [12] of the temperature dependence of Raman scattering spectra for two orientations of L-MET single crystals we were able to demonstrate the presence of two conformers of L-MET in the crystalline unit cell up to a temperature of 307 K. Above this temperature, however, the crystal undergoes a phase transition, and the conformations of the two

types of molecules A and B are modified, even though the monoclinic structure is conserved [12].

It is therefore of considerable interest to gain further understanding of the dynamics of the thiol-ether ( $\text{R}-\text{S}-\text{R}'$ ) group in this particular amino acid. Dynamics involving the H atoms can be probed by spectroscopic techniques such as Nuclear Magnetic Resonance (NMR) [13], Raman scattering (RS) [14], Infrared (IR) [14] and incoherent inelastic neutron scattering (IINS) [15] spectroscopies, which in turn are highly sensitive to the subtle structural changes that arise from changes in packing density from variations in intermolecular distances in the H-bond network. The special utility of IINS measurements on organic molecules is based on the fact that the signal is dominated by the incoherent scattering from H, which has been exploited in reports by several groups on the H-dynamics of amino acids [15–21].

In this work we add significant new information to our studies [12] of the dynamics of L-MET by combining quasielastic and inelastic neutron scattering with DFT calculations along with X-ray powder diffraction (XRPD). Our results now clearly show that the dynamical disorder observed in L-MET is indeed a result of the flexibility of the thiol-ether group. Moreover, analysis of the evolution of the methyl group dynamics with temperature provides improved understanding of the weak intramolecular interactions [22], which facilitate the subtle conformational changes, and thereby result in a great deal of complexity in the analysis of the crystal structures.

## 2. Materials and methods

### 2.1. Powder samples and single crystals

L-MET powder samples were purchased from Sigma-Aldrich and used without further purification. Possible traces of water in L-MET were analyzed by means of thermogravimetry and differential thermal analysis using a Netzsch TG 449F3 up to 620 K and a PerkinElmer instrument in the temperature range from 320 K to 470 K. No water was found to be present, however two high temperature phase transitions were clearly observed, see SI for details. Single crystals were grown by slow evaporation of an aqueous solution at 275 K. Crystals in the form of thin elongated plates of diverse sizes were obtained after three to four weeks.

### 2.2. Incoherent inelastic neutron scattering

The dynamic behavior of L-MET powder samples was studied using IINS over a wide range of time scales, from tenths of picoseconds to a few nanoseconds, using three different spectrometers, NEAT, SPHERES and IN10 at HZB (Berlin, Germany), JCMS (Garching, Germany) and ILL (Grenoble, France), respectively. To minimize the effects of multiple scattering during the INS measurements, the sample transmission was kept at 0.9.

The measured scattering function  $S(\mathbf{Q}, \omega)$ , where  $\mathbf{Q}$  is the magnitude of the scattering wave vector and  $\omega$  is the energy transfer, will express different contributions distinguishing different types of motion depending on the temperature and energy resolution (time) range.  $S(\mathbf{Q}, \omega)$  can be decomposed into three components: elastic ( $S_E(\mathbf{Q}, \omega = 0)$ ), quasi-elastic ( $S_{QE}(\mathbf{Q}, \omega \sim 0)$ ) and inelastic ( $S_{IN}(\mathbf{Q}, \omega > 0)$ ) [23] scattering. INS measurements on polycrystalline samples were carried out between 80 and 375 K using the time-of-flight (ToF) spectrometer NEAT,  $\lambda_i = 5.1\text{\AA}$ ,  $\Delta E = 98\text{ }\mu\text{eV}$ . The dynamical susceptibility [24]  $\chi''(\omega)$ , defined in Eq. (1), was calculated after elimination of detectors with intensity from diffraction peaks using the program FITMO [25],

$$\frac{\chi''(\omega)}{\omega} = \frac{1}{N_D} \sum_i S(\theta_i, \omega) \times \frac{B(\omega, T)}{|\hbar\omega|}. \quad (1)$$

$N_D$  is the total number of detectors, and  $S(\theta, \omega)$  is the scattering vector which is calculated at each energy transfer for the averaged

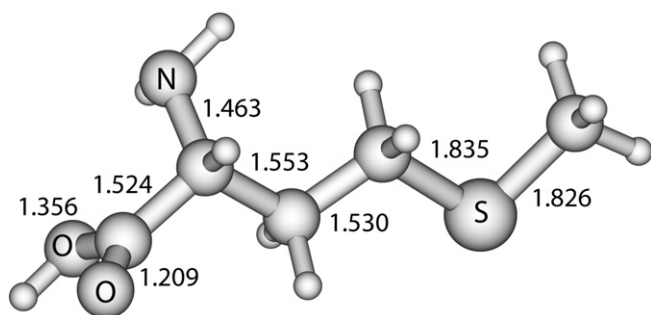


**Fig. 1.** Calculated structure of the gas phase L-MET molecule indicating the formation of two distinct C–O bond lengths of the carbonyl group. Note that the hydrogen of the  $\text{COOH}$  is transferred to the  $\text{NH}_2$  group in the crystal.

scattering angle.  $B(\omega, T)$  is a function accounting for the population of the vibrational modes with temperature. The susceptibility is obtained after an averaging over the scattering angles used in the experiment, which improves the counting statistics but smoothes the coherence effects of the scattering. This is the so-called incoherent approximation. A broader view of the different motions that can be activated in  $\iota$ -MET can be obtained by a detailed analysis of the quasielastic part of the spectra. The quasielastic spectra were also investigated using the backscattering instruments SPHERES ( $\lambda_i = 6.27 \text{ \AA}$ ,  $\Delta E = 0.65 \text{ \mu eV}$ ) and IN10 ( $\lambda_i = 6.27 \text{ \AA}$ ,  $\Delta E = 1 \text{ \mu eV}$ ) to study motions on the ns time scale. Finally, analysis of the temperature dependence of the elastic intensity,  $S_E(<Q>, \omega 0)$ , binned over the total  $Q$  range explored, makes it possible to identify relevant dynamical transitions from abrupt changes in the elastic scattering in a manner which is model-independent [26].

### 2.3. Computational details

The experimental crystal structure [10,11] was the starting structure for the optimization of the atomic positions with the lattice parameters kept fixed. Calculations on molecular  $\iota$ -MET were performed at the B3LYP/6-31G\*\* level of theory with the GAMESS-UK package [27]. The geometry was optimized and confirmed to be a genuine minimum by a Hessian calculation. The flexibility of the molecule was investigated from calculations of rotational profiles around various bonds in the gas phase molecule. This was accomplished by varying the corresponding dihedral angle from  $0^\circ$  to  $360^\circ$  in steps of  $10^\circ$ , and this angle was kept fixed during optimization of the remaining structural parameters. Periodic calculations on crystalline  $\iota$ -MET were performed with the VASP [28] package using the PBE functional along with Vanderbilt ultrasoft pseudopotentials [29] with a plane wave kinetic energy cut-off of 450 meV. A  $4 \times 4 \times 4$  Monkhorst-Pack mesh of  $k$ -points was used for the periodic calculations. The barrier to rotation for the methyl group was derived from single point energy calculations in the periodic structure, where the methyl group orientation about the S-CH<sub>3</sub> axis was incremented in  $5^\circ$  steps in a frozen atom approach. Differences between the gas phase and periodic calculations of the methyl barrier to rotation are discussed in detail below.

### 2.4. X-ray powder diffraction

Variable-temperature X-ray powder diffraction, XRPD, studies of  $\iota$ -MET were carried out between 100 and 375 K using a Bruker D8 Advance Diffractometer with CuK $\alpha$  radiation,  $\lambda = 1.5418 \text{ \AA}$  in  $\theta/\theta$ -geometry equipped with a Bruker Lynx Eye position sensitive detector, PSD, which makes it possible to do measurements in a very short time without loss of resolution. A TC wide range temperature chamber (MRI Physikalische Geräte GmbH), which can operate between 83 K and 723 K, was used for the variable-temperature measurements. A  $2\theta$  range from  $5^\circ$  to  $60^\circ$  was covered using a step of  $0.0126^\circ$  and a counting time of 53 s. The evolution of the main Bragg-peak located between  $22.5^\circ < 2\theta < 25.5^\circ$  was monitored using a scan with fixed PSD (position sensitive detector) on cooling from room temperature to 130 K and again on heating up to room temperature. The powder diffraction data were analyzed using the program FullProf [30].

## 3. Results and discussion

### 3.1. Temperature dependence of the vibrational spectra

We begin by reviewing some of the results of detailed Raman spectra of  $\iota$ -MET reported by us in a recent publication [12]. Therein we proposed a relatively complete assignment of the vibrational modes of crystalline  $\iota$ -MET based on a limited number of literature reports of vibrational spectroscopic studies, ab initio calculations of

$\iota$ -MET [31–34] and our own Raman spectroscopic studies and attendant calculations. This also took into account results from THz time-domain spectroscopy [33], which suggest that the C $\beta$ –C $\alpha$  torsion,  $\tau(\text{C}_\beta - \text{C}_\alpha)$ , and the S–CH<sub>3</sub> deformation,  $\delta(\text{S}-\text{CH}_3)$ , modes in  $\iota$ -MET are located around 30 and 60 cm<sup>−1</sup>, as well as the general finding [35–39] in amino acids that the lattice modes and the torsion of the CO<sub>2</sub><sup>−</sup> group,  $\tau(\text{CO}_2^-)$  are expected below 200 cm<sup>−1</sup>. Differences between observed frequencies and those calculated for the isolated molecule were shown to arise mainly from the fact that the hydrogen of the COOH group is transferred to the NH<sub>2</sub> group in the crystal (Fig. 1) so that the C–O bond lengths of the carbonyl group are almost identical in the crystal with a bond length around 1.3 Å, while two distinct bond lengths of 1.21 Å and 1.36 Å are found for the free molecule [12].

We now turn to the low frequency range of the vibrational spectra of  $\iota$ -MET, where better insight can be gained from the IINS spectra. Because of the large incoherent scattering cross section of hydrogen, the inelastic scattering function  $S(Q, \omega)$  corresponds to a good approximation to those molecular vibrations involving displacements of the H-atoms. Resolution of IINS spectra is, however more limited, than that in RS and IR spectroscopy. Moreover, thermal motion (Debye Waller factor) has a significant effect on the IINS spectra so that the IINS spectrum is dominated by anti-Stokes scattering, and will obey the Bose–Einstein statistics [40]. On the other hand, the use of the NEAT spectrometer in neutron energy gain makes it possible to follow the evolution of the quasielastic part of the dynamical response over an unrestricted temperature range in addition to the evolution of the lattice vibrations on cooling down to 100 K, as well as the vibrational spectra to temperatures as low as about 150 K.

The temperature dependence of the vibrational spectra in the form of the dynamical susceptibility,  $\chi''(\omega)$ , of  $\iota$ -MET obtained using expression (1) is shown in Fig. 2(a), along with the IINS spectrum obtained [41] from the atomic displacements and frequencies of the VASP calculation, Fig. 2(b). The nature of a particular vibrational mode can be assessed by visual inspection of the atomic displacements involved (e.g. with the use of Jmol [42]). The low frequency modes are, of course, largely coupled and of collective character. The most prominent bands in the INS spectrum at 110 K near 83 cm<sup>−1</sup>, for example, involves a skeletal twisting motion with rocking of the –CH<sub>2</sub> groups, i.e. large displacements of many H atoms. The other intense band in the INS at about 200 cm<sup>−1</sup> contains several modes including  $\delta(\text{S}-\text{CH}_3)$  calculated to be at 191 cm<sup>−1</sup>, CO<sub>2</sub> torsional (186 cm<sup>−1</sup>) and rocking motions coupled with skeletal deformations which also involve H atom displacements. The somewhat less intense band near 140 cm<sup>−1</sup> appears to have its origin in C–S–C deformation modes. Another mode of interest in the current study is the methyl torsion about the S–C bond, which is found around 330 cm<sup>−1</sup> in the periodic VASP calculation. Since frequencies calculated by standard quantum chemistry programs are, however, harmonic, it is likely that the highly anharmonic methyl torsional motion occurs at somewhat lower frequencies, even though the IINS spectrum at 140 K exhibits a fairly strong band in this region of the spectrum. We tentatively propose that this mode is likely to be assigned to the strongest component of the broad and structured band around 200 cm<sup>−1</sup>, because the methyl torsion is normally one of the most intense bands in an IINS spectrum. We will see below in the discussion of the temperature dependence of the quasielastic response that this assignment is more consistent with the results presented therein than a torsional frequency of 330 cm<sup>−1</sup> would be.

Above the phase transition observed in the region 310 K  $< T <$  375 K in earlier calorimetric measurements [12,43,44] well defined peaks from vibrational modes are virtually absent in our IINS spectrum. This type of spectrum arises from the presence of a significant degree of structural disorder above room temperature combined with very large thermal motion of the molecules, which most likely include conformational rearrangements [12] and the attendant displacements of the H atoms that dominate the IINS intensities. This picture of the molecular

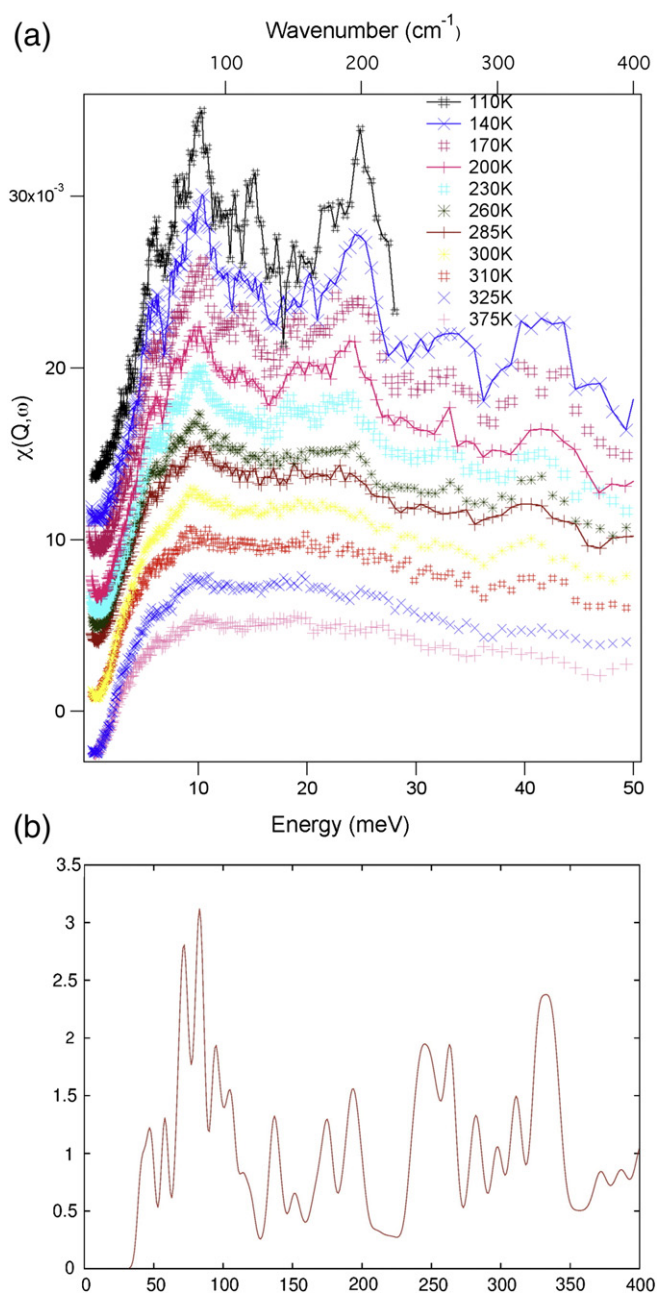


**Fig. 2.** (a) Experimental IINS spectrum (dynamical susceptibility) from 0.5 meV to 50 meV. Changes from 300 K to 375 K appear to be rather small, but much more noticeable between 300 K and 230 K. Additional changes are seen to occur between 230 K and 170 K. (b) INS spectrum obtained from frequencies and displacements given by the VASP calculation (0 K).

structure of the *l*-MET crystal at high temperatures is further supported by the powder diffraction studies described below.

The IINS spectrum appears to change gradually upon cooling from 300 K to 230 K. Such a continuous change confirms our recent Raman results, where the broad room temperature phase transition in *l*-MET between approximately 180 and 350 K with a maximum in the heat capacity at 307 K, results in a more ordered arrangement of the *l*-MET molecules [12]. Below the phase transition, i.e. from 170 K down to the lowest temperature in this experiment of 110 K, the intensities of some of the vibrational modes appear to increase more rapidly. This observation is in accord with the strong temperature dependence usually exhibited by libronic excitations [45].

### 3.2. Phase transitions and memory effect

Some more detailed information on likely structural rearrangements underlying the observed temperature dependence of the vibrational spectra were obtained by XRPD studies on *l*-MET over the temperature range of 100 to 375 K. Partial XRPD patterns of *l*-MET for selected temperatures and  $2\theta$  values from  $5^\circ$  to  $40^\circ$  are shown in Fig. 3. The dashed vertical lines in the figure indicate the expected positions of the Bragg reflections for the published structure with the  $P2_1$  space group [11] calculated for the full description of the structure at 120 K using the code FullProf. Only the cell parameters were refined at each temperature for this analysis without varying the atom positions or refining the diffraction peak shape. The final refined parameters obtained at a particular temperature were used as input parameters for the next higher temperature and so on starting with the 100 K data. It was not possible, however, to obtain the correct intensities for the diffraction peaks in the course of the structure refinement of *l*-MET. Possible effects of grain size and preferred orientation were considered since the particles of the powder sample consisted of somewhat large, elongated plates. Grinding of the sample did not, however, lead to a structural change as observed, for instance, for DL-cysteine [25]. Furthermore, it is important to note that the [001]-reflection ( $2\theta \sim 5.8^\circ \pm 0.1^\circ$  at 120 K) exhibits a highly asymmetric lineshape (see insets in Fig. 3), even though it is indexed as a unique reflection [12] in the  $P2_1$  space group. This Bragg peak may well consist of more than one peak over the entire temperature range of our analysis. This observation strongly suggests that either the  $P2_1$  structure is not correct or that more than one phase is present. This question cannot, however, be resolved from the limited powder diffraction data we have which are available, and would require extensive temperature dependent single crystal neutron diffraction studies.

While it was not possible to carry out a more complete structural analysis because of problems with data and sample quality, as well as the complexity of the  $P2_1$  space group, cell parameters and cell volume within the  $P2_1$  space group could be analyzed over the entire temperature range as described above. Rather different trends can be distinguished in phases I and II, i.e. below and above the small anomaly observed in the specific heat [12] at about 220 K. On heating we observe (Fig. 4) an anomalous drop of the *c*-lattice parameter at around 190 K, which is followed by a linear increase upon further heating. The  $\beta$ -angle is also observed to decrease abruptly at the same temperature. Another striking feature revealed by the XRPD experiments is the continuous increase of the *b*-lattice parameter on cooling from room temperature with a small decrease near 250 K. Such negative thermal expansion along one particular crystallographic direction has been reported for many molecular crystals, such as NMA [28], organic conductors, such as (TMTTF)<sub>2</sub>X [29], molecular crystals, such as, methanol monohydrate [30], and amino acids, such as *l*-alanine [31], and has been interpreted to be the result of anharmonicity of the interatomic potential. The expansion of the *c*-axis in *l*-MET is found to be 10 times greater than that of the *a*-axis, which is consistent with the fact that the structure is layered perpendicular to the *c*-direction. These changes in the crystallographic data can then be directly connected to the second, small anomaly observed at about 220 K in the  $C_p$ -measurements on powder samples.

Anomalies observed in the structural parameters were further explored by scanning the intensities of selected reflections ([004], [02], [112]) on cooling to 130 K and subsequent heating to 300 K with a fixed position-sensitive detector (PSD) at a continuous cooling rate of 2 K/min. These measurements confirm, (Fig. 5), that below 250 K there is a change in the evolution of the intensities of the peak followed by another change below 180 K. These temperatures noticeably correspond, respectively, to anomalies observed in the  $C_p$  data [12] and the maximum in the unit cell volume. We also find that the crystalline structure is strongly dependent on thermal history of the sample. We observe (Fig. 4) that the peak at  $23.4^\circ$ , indexed mainly as the [004] reflection, shows an interesting hysteresis after a cycle of

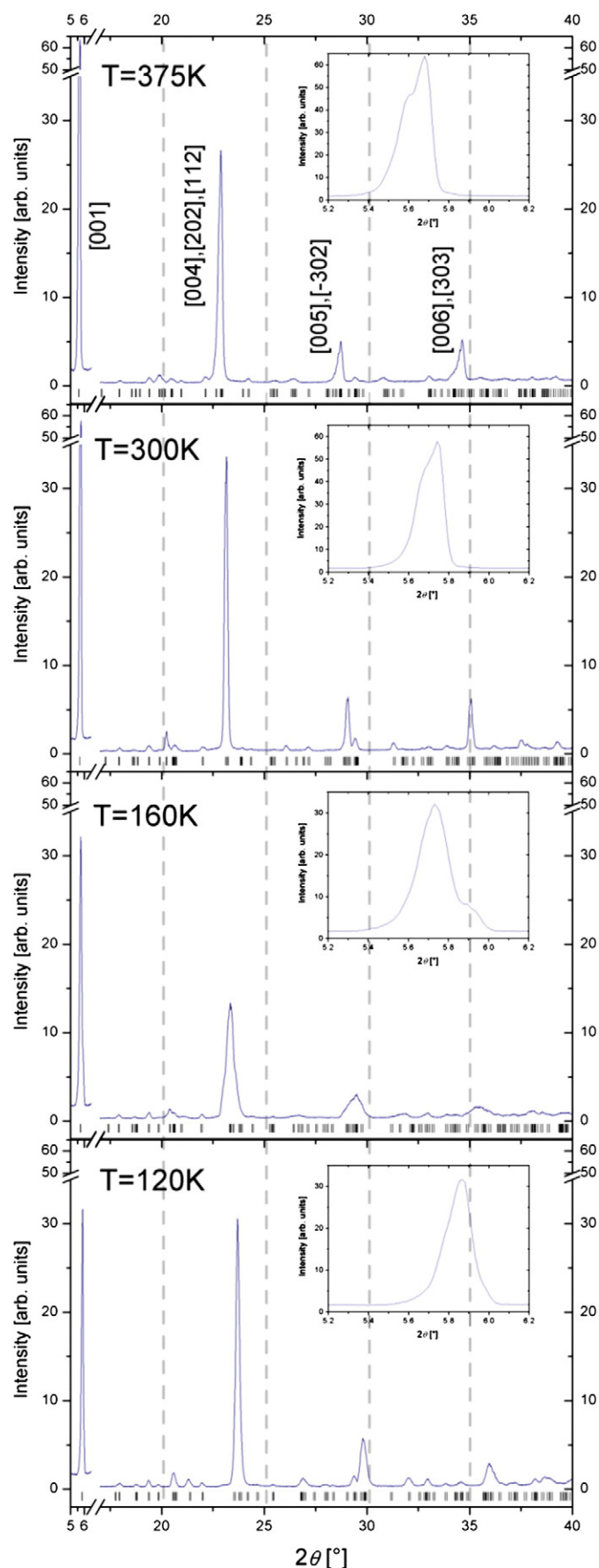


**Fig. 3.** X-ray diffraction pattern in the  $2\theta$ -region from  $5^\circ$  to  $40^\circ$  at 120, 160, 300 and 375 K. The markers indicate the Bragg reflections for the  $P2_1$  structure obtained from the structural refinement described in the text. The inset shows the [001]-reflection in greater detail.

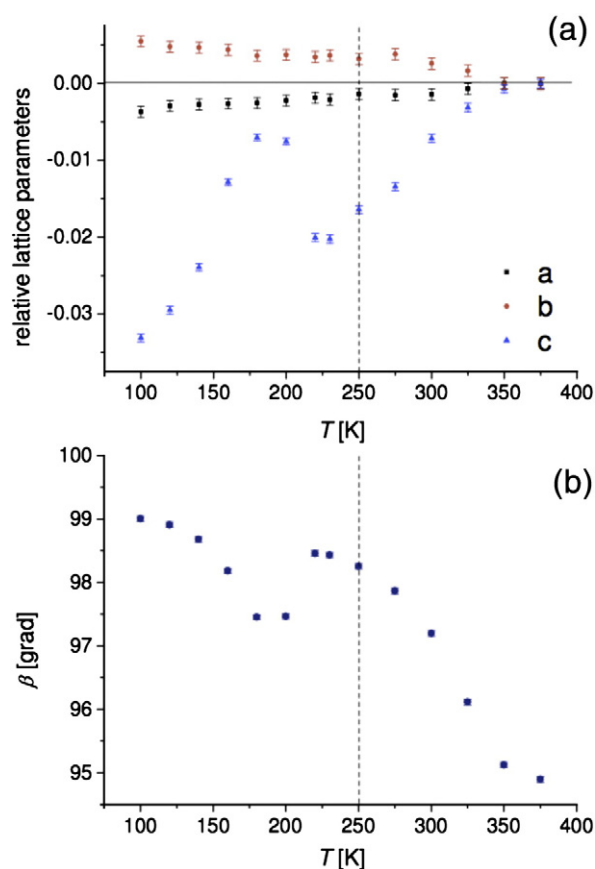


**Fig. 4.** (a) Lattice constants of l-MET determined by Rietveld refinements with fixed atomic positions in the monoclinic cell [11]. The lattice parameters are shown as a percent change with respect to measurements at 375 K (e.g.  $\Delta a(T) = [a(T) - a(375\text{ K})]/a(375\text{ K})$ ), while their values at 375 K are  $a = 9.5444(9)\text{Å}$ ,  $b = 5.1802(1)\text{Å}$  and  $c = 15.535(5)\text{Å}$ . Errors are calculated in the Gaussian approximation, while errors of lattice parameters are obtained from the Rietveld refinement. (b) Evolution of the  $\beta$ -angle for monoclinic l-MET as a function of temperature. The horizontal lines are guides to the eyes, while the vertical dotted line indicates the temperature separating phases I and II.

cooling down to 130 K and heating back to 300 K. The same reflection is then found at an angle of  $22.9^\circ$ , which differs from the initial position by  $0.5^\circ$ , or a change in the c-lattice parameter of  $0.32\text{ Å}$  (2%). Possible structural relaxation phenomena upon cooling the sample were investigated by means of a scan with fixed PSD every 20 s at constant temperature of 300 K following the temperature cycling. The intensity of the peak located at  $2\theta = 22.9^\circ$ , marked by an arrow in Fig. 4, was fitted with a Gaussian at each time step with the result that its time dependence (Fig. 4(c)) reveals that l-MET relaxes back to its initial (or equilibrium) state at 300 K within 15 min. A comparison of the diffraction patterns from  $2\theta = 5^\circ$  to  $60^\circ$  taken before the fixed PSD scan to the one taken afterwards following a wait of 15 min at room temperature confirms this observation. These reversible structural changes differ markedly, for example, from those reported for taurine, a non-essential amino acid that can be synthesized in the human body from methionine via cysteine, where an irreversible change in the crystal was shown to be induced by irradiation from a conventional X-ray tube at 87 K [32].

While we can clearly observe (Fig. 3) distinct but somewhat broadened Bragg-peaks in the X-ray diffraction patterns up to 375 K in polycrystalline l-MET, the high temperature dynamics suggest that l-MET is in fact in a dynamically highly disordered state down to 310 K. Thus we can argue that the crystalline structure of l-MET evolves upon cooling from a dynamic arrangement with a wide distribution of H-bonds to a more stable system characterized by stronger

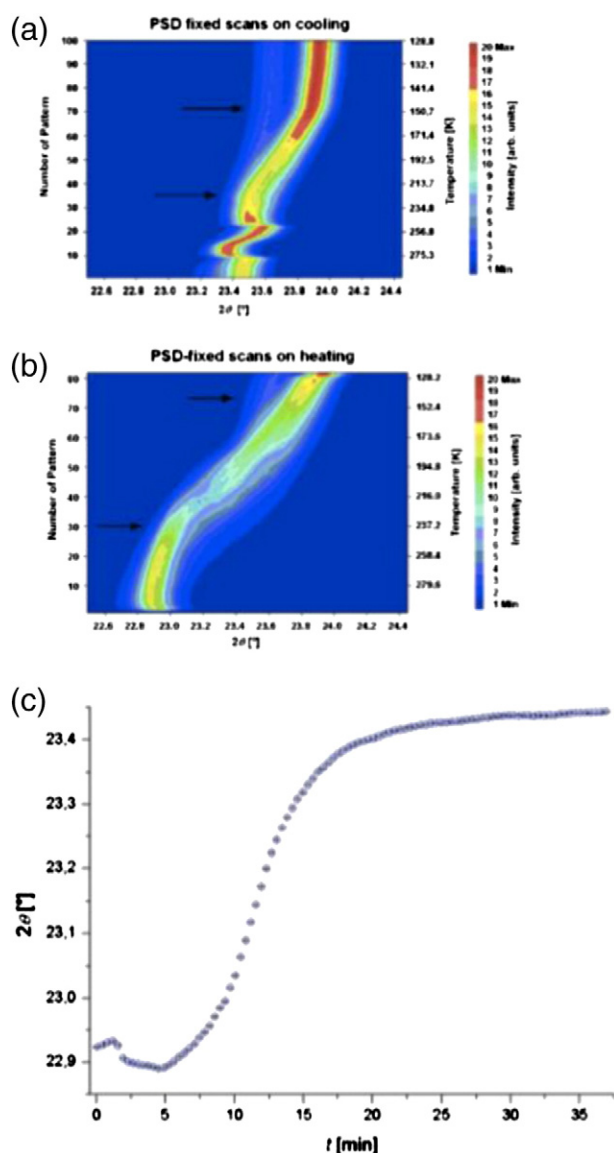


**Fig. 5.** (a) Scan with fixed PSD shows a smooth change on cooling in the peak position versus temperature around 220 K and around 150 K. (b) The same type of scan on heating shows the transitions around 240 K and 150 K as well. (c) After cooling the sample to 130 K and subsequent heating to room temperature the scan at constant temperature shows an intriguing time dependence of the structure.

intermolecular hydrogen bonds. Such a structural relaxation can occur at ambient temperatures because the material may exhibit differences in the local structure which gives rise to some dynamic disorder. The latter may result from a distribution of low energy barriers and a range of intrinsic times, which limits molecular motions, while the time average structure of L-MET still appears to be quite crystalline. We may thus conclude that the changes in the overall structure of phase I are related to variations of the interactions of the L-MET molecules with the crystalline environment most likely of dynamic origin as was previously observed in L-alanine [46] and L-cysteine [47]. This idea is further supported by the examination of the peak shapes (Fig. 3), where Bragg-peaks between 250 and 160 K are broader when compared to the patterns at higher and lower temperatures. Since interactions leading to conformational changes are small, the changes in the system energy may be barely detected in a DSC experiment, and most likely observable in the  $C_p$ , but they are expected to clearly manifest themselves in the dynamical measurements over a broad energy range.

### 3.3. Slow dynamics in L-methionine

Further insight into the nature of the possible local conformational transitions induced by thermal activation can be gained in a number of ways using the elastic energy window of various spectrometers we used. Time scales of the dynamics of side groups can thereby be selected within a range of four decades in time (0.2 ps–2 ns) in our experiments. Quasielastic scans over a wider energy range on these instruments can then more specifically measure line broadening as a function of temperature.

No such quasielastic broadening of the elastic line, nor any low energy inelastic excitations indicative of either tunneling of the  $\text{CH}_3$  or  $\text{NH}_3$  groups or of soft phonon modes are, however apparent in the neutron scattering spectrum at the lowest energies ( $-10 \mu\text{eV} < \omega < 10 \mu\text{eV}$ ) recorded at temperatures of 3 and 300 K on the backscattering spectrometer SPHERES at the FRM-II (Fig. 6(a)). We may therefore conclude that all molecular motions are frozen at 3 K on the time scale given by the instrumental resolution. A very weak quasielastic signal may be evident at 300 K, but this contributes mainly to the background of the spectrum and therefore cannot be further analyzed. A fixed-window temperature scan (Fig. 6(b)) of the elastic intensity ( $\Delta E = 1 \mu\text{eV}$ , or 0.25 GHz) reveals that two breaks in the straight line decrease from generally increasing thermal motion, namely at temperatures of 130 K and 275 K. These changes in slope indicate that scattering from some dynamical process becomes fast enough to shift more intensity outside the elastic window. A similar scan with a much larger window, that of elastic intensity,  $S_E(Q, \omega = 0)$  summed over the entire  $Q$  range on the NEAT spectrometer with  $\Delta E = 98 \mu\text{eV}$  or 24 GHz (Fig. 6(c)) shows just one of these breaks from linearity, namely the one at about 275 K. The two changes in slope occur at rather high temperature and may therefore be attributed to the onset of rapid reorientational motion by some parts of the molecule over barriers of two different heights. The onset of what has been described as stochastic reorientation of the methyl group, for example, causes a drop in the elastic intensity because of the fact that such quasielastic broadening from faster  $\text{CH}_3$  reorientations gradually moves outside of the elastic energy window of the backscattering spectrometer as the temperature increases. This signal becomes so broad as to be nearly flat at temperatures above 130 K. We note, however, that the changes in the cell parameters observed by XRPD in the region about 220 K do not appear to have an obvious signature in the dynamics shown by these fixed window scans.

The origin of this quasielastic broadening may in principle be determined from its direct observation with the NEAT spectrometer, as it can be seen to emerge at temperatures between 110 K and 140 K and to increase in intensity and width upon further heating (Fig. 6(d)). The geometry of the observed motion could not, however, be ascertained because the weakness of this signal made it impossible to analyze its dependence on  $Q$ . These quasielastic spectra could still be analyzed by summing the data over  $Q$ , which then provides a qualitative description of the temperature dependence in terms of a single Lorentzian line width. It is customary to relate the half-width at half-maximum (HWHM) of the quasielastic Lorentzian (Fig. 6(e)) to an effective activation energy for the process giving rise to this scattering by the Arrhenius relation [23]:  $\Gamma = \Gamma_0 e^{-E_{\text{act}}/kT}$ , where  $\Gamma_0$  and  $E_{\text{act}}$  are the attempt frequency and the apparent activation energy, respectively. Such a fit over the region below 275 K results in an activation energy  $E_{\text{act}} = 1.6 \pm 0.3 \text{ kJ/mol}$  for the motion that gives rise to this quasielastic broadening along with an attempt frequency  $\Gamma_0 = 2.27 \pm 0.01 \text{ meV}$ .

The time scale of this process (a HWHM as large as 0.2 meV) places it well in context with what is typically observed for the reorientation of methyl groups in a wide variety of systems [48] so that we can readily attribute it to the  $\text{S}-\text{CH}_3$  group in L-MET. We note, however, that the temperature dependence of the HWHM of quasielastic scattering from reorienting methyl groups has been observed to tend to a common value (corresponding to a methyl hopping rate of about  $10^{12} \text{ s}^{-1}$ ) at

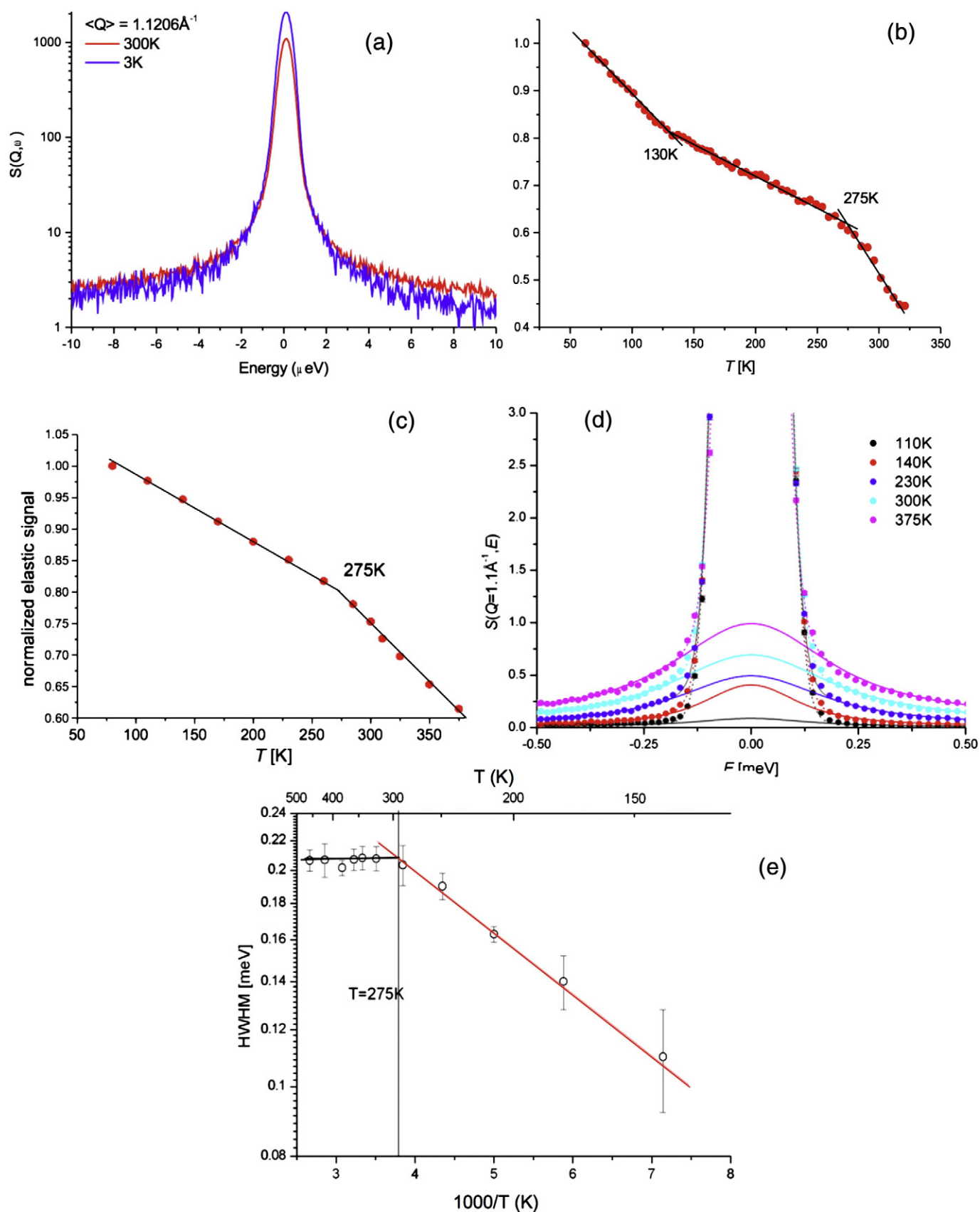


**Fig. 6.** (a) Quasi-elastic signal averaged over the full  $Q$ -range at 3 K and 300 K measured on SPHERES at FRMII, shows a small quasi-elastic signal at 300 K mainly in the background. (b) Normalized elastic signal obtained using IN10 with  $\Delta E = 1 \mu\text{eV}$  as a function of temperature showing two dynamical transition at about 130 and 275 K. (c) Normalized elastic signal obtained using NEAT with  $\Delta E = 98 \mu\text{eV}$  as a function of temperature showing a dynamical transition at about 275 K. (d) Dynamic structure factors obtained using NEAT for  $\Delta E = 98 \mu\text{eV}$  at selected temperatures. The data were averaged over the full  $Q$ -range. The experimental spectrum ( $\bullet$ ) is shown together with the best fit (solid line). (e) Evolution of the half-width at half-maximum (HWHM) of the Lorentzian function fitted to the quasielastic signal versus temperature showing a plateau above 275 K.

high temperatures, while in the present case it is seen to be level above 275 K. This suggests that the crystalline structure of L-MET is dynamically highly disordered above 275 K and that extensive coupling between the moieties CH<sub>3</sub>, NH<sub>3</sub>, and CO<sub>2</sub>, results in a dynamically rather homogeneous system. This picture is also reflected by our high temperature Raman and INS spectra and by the X-ray powder diffraction results. Increases of low-frequency scattering clearly observed in the Raman spectra [12] as well as in the IINS spectra (Fig. 2), may be related to this second discontinuity at around 275 K in the elastic-scan data, and consequently we may argue that this quasielastic broadening helps understand the unusual increases of the low-frequency Raman scattering of L-MET as compared to that in other crystalline amino acids.

We can attempt to verify that the motion observed on the ps time scale in the temperature range from 275 K to 140 K does in fact originate from reorientations of the methyl group by relating the observed activation energy to details of the rotational PES and transitions of the methyl group. From an analysis of the calculated barrier heights (Table 1, Fig. 7), one can estimate the effective barrier to rotation methyl group about the S–CH<sub>3</sub> axis in L-Met to be about 7.5 kJ/mol (77 meV). This calculation was, however, performed on the isolated molecule, so that actual barrier to rotation in the crystal may be appreciably higher than this value on account of the intermolecular interactions. This difference has been determined in a number of cases [49], and can be taken to be approximately 2.0 kJ/mol for total barrier height of 9–10 kJ/mol in L-Met. The shape of the rotational PES has to be known, however, in order to relate the barrier height to rotational transitions. While a 3-fold PES is normally a good starting point for methyl rotation, the results from our calculation suggest that higher order terms (6-fold, etc.) may be needed to accurately describe the PES. If we take the effective rotational barrier height to be about 100 meV, we find that the 0–1 librational transition would occur at 22.6 meV (182 cm<sup>−1</sup>), and the tunnel splitting would be 0.015 μeV for a PES with purely 3-fold rotational symmetry, or 40 meV and 25 μeV, respectively, if the PES were purely 6-fold. Our tentative assignment of the methyl torsion to the strongest peak in the INS at about 200 cm<sup>−1</sup> would then suggest that the PES is mostly of 3-fold nature with perhaps as much as a 10% modulation with a six-fold term. The attendant tunneling transitions would not be observable with SPHERES in accord with our results (Fig. 6(a)).

We have investigated the effect of intermolecular interactions on the PES for methyl reorientation using a frozen atom approach within our periodic VASP calculation, as described above, and found it to be 121 meV. For a 3-fold PES with such a barrier height the librational transition would be at 201 cm<sup>−1</sup>. We might expect this value of the barrier to rotation to be too high as some relaxation of the molecular structure would also occur in the solid, and act to lower this barrier. It therefore seems quite plausible that the actual barrier to rotation falls somewhere between the estimate derived above (appr. 100 meV) and the one calculated in the frozen atom approximation for the crystal.

While it would seem reasonable to relate the effective activation energy for reorientation of the methyl group over the range from 130 to 275 K of 1.6 kJ/mol obtained above to details of the PES for the methyl group, most notably the actual barrier height, this would only be appropriate if methyl reorientation over this entire temperature range were purely classical. It has, however, become clear in recent years that this limit is not reached, and that these dynamics are partly of quantum

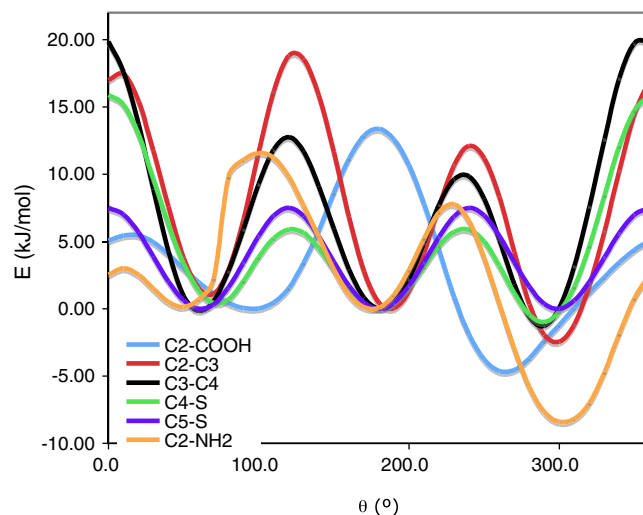


Fig. 7. Computed rotational profiles around the various bonds for the gas-phase molecule.

mechanical nature [50,51] even at room temperature. A partial loss of quantum coherence is expected to occur as the temperature is increased with the effect that the rotation becomes increasingly incoherent [52] and this process can be governed by a different rate constant from that for the coherent rotation.

Finally we need to return the second break in the ns time scale (high resolution) temperature scans (Fig. 6(b)) at 275 K, which indicates the onset of additional broadening from processes slower than the methyl reorientation. These may then be taken to be the reorientations about one or more bonds of the backbone of the molecule, which in turn give rise to the distribution of methyl PES's indicated by the flattening of the temperature dependence of the methyl reorientation rate above 275 K (Fig. 6e).

We can therefore conclude that the quasielastic signal characterizing the fast processes of order ps, i.e. the reorientations of the methyl group, which is observed far below the high temperature phase transition, acts as precursor for the conformational changes in L-MET which occur on the ns time scale above 275 K. The discontinuities in the temperature dependence of the normalized elastic signal correlate well with our Raman scattering results [12] and hence are indicative of conformational changes involving motions on different time scales. Therefore, we may propose that the available thermal energy can no longer be accommodated by molecular librations alone, and this thermal energy is transferred to the lattice, leading to the instability and consequently the phase transition at 307 K.

#### 4. Conclusion

We have been able to identify the origin of the conformational flexibility of the side chain in crystalline L-MET by combining inelastic and quasielastic neutron scattering, and X-ray powder diffraction with DFT calculations along with our previously reported Raman scattering study [12]. The results presented here highlight the apparent existence of multiple minima on the L-MET potential surfaces in a similar form as observed for example in globular proteins. This finding is corroborated by the occurrence of reorientational motions around various bonds of the molecule on the ns and ps time scales at certain temperatures along with our previously reported observation of intensity changes in particular Raman bands, which can only be explained if at least one of the two L-MET conformers in the monoclinic unit cell changes configuration. Such reorientational motions contribute to lattice instabilities and, consequently the occurrence of the structural changes shown by thermal analysis. The temperature

Table 1  
Estimates of the rotational barriers around the different single bonds in MET.

Bond	E <sub>act</sub> (kJ/mol)	Bond	E <sub>act</sub> (kJ/mol)
C <sup>2</sup> –COOH	18.0	C <sup>4</sup> –S	16.9
C <sup>2</sup> –C <sup>3</sup>	21.3	C <sup>5</sup> –S	7.5
C <sup>3</sup> –C <sup>4</sup>	21.1	C <sup>2</sup> –NH <sub>2</sub>	20.0

dependence of the IINS spectra suggests that the reorientational dynamics of the S-CH<sub>3</sub> and CO<sub>2</sub> moieties, and consequently of the NH<sub>2</sub> group, are triggered as a cascade of thermal activated events, i.e. that the motions are unlocked sequentially, leading to a convoluted disordered H-bonded network at room temperature. As a result polycrystalline L-MET seems to be in a dynamic glassy-like state down to 310 K with well-defined crystallinity, which evolves upon cooling, from an arrangement possessing a large fluctuating distribution of H-bonds to a more homogeneous system stabilized by stronger intermolecular H-bonds.

Our findings relate to the role of L-methionine in binding/recognition of hydrophobic ligands (lipids) and its binding to atoms such as metals, especially because it is a hydrophobic amino acid, and therefore deeply buried inside of the protein structure. We can therefore expect that its properties in the solid state will not differ appreciably from that in aqueous so that the description of the dynamics given in the present work, particularly with regard to the flexible S-CH<sub>3</sub> group, can be factored into that for macromolecules, which contain this very common linker. This may well include the extremely interesting phase transition we observe in L-Met at body temperature at around 310 K.

### Author contributions

The manuscript was written with contributions of all authors. All authors have given approval to the final version of the manuscript.

### Acknowledgment

Part of the results presented in this work were obtained during the development of the Diplomarbeit of JF at the University of Kassel, and financially supported by the Helmholtz-Zentrum Berlin (HZB) through the groups of Prof. Dr. M. Ballauff and Dr. A. Kyriakopoulos. JF acknowledges Andrey Maljuk (HZB) for the thermal measurements. JF and HNB thank Tilo Seydel (ILL) and Joachim Wuttke (JCNS) for the support during the IN10 and SPHERES experiments, respectively. JE would like to thank Jernej Stare (NIC, Slovenia) for the help with some of the computational aspects. HNB would also like to acknowledge Mark Johnson (ILL) for the helpful discussions. This research was financed by FUNCAP, CNPq and by the Deutsche Forschungsgemeinschaft (DFG project GZ: 444 BRA-113/310/0-1). RWAH acknowledges the Netherlands Organisation for Scientific Research (NWO/ECHO), grant 700.57.027. The support given by the Berlin Neutron Scattering Center (BENSCH), Institut Laue-Langevin (ILL) and Jülich Center for Neutron Scattering (JCNS) is also acknowledged.

### Appendix A. Supplementary data

Details on DSC measurements at high temperature showing the existence of two phase transitions. Supplementary data to this article can be found online at doi: <http://dx.doi.org/10.1016/j.bpc.2013.06.011>.

### References

- [1] J.T. Brosnan, M.E. Brosnan, The sulfur-containing amino acids: an overview, *Journal of Nutrition* 136 (2006) 1636S–1640S.
- [2] S.H. Gellman, On the role of methionine residues in the sequence-independent recognition of nonpolar protein surfaces, *Biochemistry* 30 (1991) 6633–6636.
- [3] H.J. Drabkin, U.L. Rajbhandary, Initiation of protein synthesis in mammalian cells with codons other than AUG and amino acids other than methionine, *Molecular and Cellular Biology* 18 (1998) 5140–5147.
- [4] T. Meinel, Y. Mechulam, S. Blanquet, Methionine as translation start signal: a review of the enzymes of the pathway in *Escherichia coli*, *Biochimie* 75 (1993) 1061–1075.
- [5] J. Moskovitz, Methionine sulfoxide reductases: ubiquitous enzymes involved in antioxidant defense, protein regulation, and prevention of aging-associated diseases, *Biochimica et Biophysica Acta, Proteins and Proteomics* 1703 (2005) 213–219.
- [6] R.L. Levine, L. Mosoni, B.S. Berlett, E.R. Stadtman, Methionine residues as endogenous antioxidants in proteins, *PNAS* 93 (1996) 15036–15040.
- [7] S. Luo, R.L. Levine, Methionine in proteins defends against oxidative stress, *The FASEB Journal* 23 (2009) 464–472.
- [8] H.D. Bernstein, M.A. Poritz, K. Strub, P.J. Hoben, S. Brenner, P. Walter, Model for signal sequence recognition from amino-acid sequence of 54 K subunit of signal recognition particle, *Nature* 340 (1989) 482–486.
- [9] B. Khawas, The unit cells and space groups of L-methionine, L-β-phenylalanine, and D-tyrosine, *Acta Crystallographica B26* (1970) 1919–1922.
- [10] K. Torii, Y. Iitaka, Crystal structures and molecular conformations of L-methionine and L-norleucine, *Acta Crystallographica B29* (1973) 2799–2807.
- [11] B. Dalhus, C.H. Görbitz, Crystal structures of hydrophobic amino acids. I. Redeterminations of L-methionine and L-valine at 120 K, *Acta Chemica Scandinavica* 50 (1996) 544–548.
- [12] J.A. Lima Jr., P.T.C. Freire, F.E.A. Melo, J. Mendes Filho, J. Fischer, R.W.A. Havenith, R. Broer, H.N. Bordallo, Using Raman spectroscopy to understand the origin of the phase transition observed in the crystalline sulfur based amino acid, *Vibrational Spectroscopy* 65 (2013) 132–141.
- [13] R. Ishima, D.A. Torchia, Protein dynamics from NMR, *Nature Structural Biology* 7 (2000) 740–743.
- [14] R. Schweitzer-Stenner, Advances in vibrational spectroscopy as a sensitive probe of peptide and protein structure: a critical review, *Vibrational Spectroscopy* 42 (2006) 98–117.
- [15] H.N. Bordallo, M. Barthès, J. Eckert, Vibrational dynamics of crystalline L-alanine, *Physica B: Condensed Matter* 1138 (1997) 241–243.
- [16] A. Pawlukojć, J. Leciejewicz, A.J. Ramirez-Cuesta, J. Nowicka-Scheibe, L-Cysteine: neutron spectroscopy, Raman, IR and ab initio study, *Spectrochimica Acta Part A: Molecular and Biomolecular Spectroscopy* 61 (2005) 2474–2481.
- [17] Y. Zhang, P. Zhang, R.C. Ford, S. Han, J. Li, Inelastic neutron scattering studies of the interaction between water and some amino acids, *Journal of Physical Chemistry B109* (2005) 17784–17786.
- [18] S.F. Parker, H.P. Harris, Inelastic neutron scattering spectroscopy of amino acids, *Spectroscopy* 22 (2008) 297–307.
- [19] J.H. da Silva, J.A. Lima Jr., P.T.C. Freire, V. Lemos, J. Mendes Filho, F.E.A. Melo, P.S. Pizani, J. Fischer, B. Klemke, E. Kemner, H.N. Bordallo, Raman spectroscopy and inelastic neutron scattering study of crystalline L-valine, *Journal of Physics: Condensed Matter* 21 (2009) 415404.
- [20] P. Chatzigeorgiou, N. Papakonstantopoulos, N. Tagaroulia, E. Pollatos, P. Xynogalas, K. Viras, Solid-solid phase transitions in DL-norvaline studied by differential scanning calorimetry and Raman spectroscopy, *Journal of Physical Chemistry B114* (2010) 1294–1300.
- [21] S.F.A. Kettle, E. Lugwisha, J. Eckert, N.K. McGuire, Intermolecular vibrational coupling in glycine, *Spectrochimica Acta A45A* (1989) 533–537.
- [22] M.R. Johnson, G.J. Kearley, Quantitative atom-atom potentials from rotational tunneling: their extraction and their use, *Annual Review of Physical Chemistry* 51 (2000) 297–321.
- [23] M. Bée, Quasielastic Neutron Scattering: Principles and Applications in Solid State Chemistry, Biology and Materials Science, Adam Hilger, Bristol, 1988.
- [24] H. Schober, Spectroscopie neutronique: un outil idéal pour le scientifique des matériaux, *Journal de Physique IV* 103 (2003) 173–202.
- [25] J. Fitter, User Manual for FITMO (NEAT TOF-Data Analysing Programme), HMI, Berlin, 1997.
- [26] B. Frick, L.J. Fetters, Methyl group dynamics in glassy polyisoprene: a neutron backscattering investigation, *Macromolecules* 27 (1994) 974–980.
- [27] M.F. Guest, I.J. Bush, H.J.J. van Dam, P. Sherwood, J.M.H. Thomas, J.H. van Lenthe, R.W.A. Havenith, J. Kendrick, The GAMESS-UK electronic structure package: algorithms, developments and applications, *Molecular Physics* 103 (2005) 719–747.
- [28] G. Kresse, J. Furthmüller, Efficient iterative schemes for *ab-initio* total energy calculations using a plane-wave basis set, *Physical Review B* 54 (1996) 11169–11186.
- [29] D. Vanderbilt, Self-consistent pseudopotentials in a generalized eigenvalue formalism, *Physical Review B* 41 (1990) 7892–7895.
- [30] J. Rodriguez-Carvajal, FULLPROF: a program for Rietveld refinement and pattern matching analysis, Abstracts of the Satellite Meeting on Powder Diffraction of the XV Congress of the IUCr, 1990.
- [31] D.J. Garfinkel, Raman spectra of amino acids and related compounds. XII. Various amino acids derived from proteins and creatine, *Journal of the American Chemical Society* 80 (1958) 3827–3831.
- [32] B.B. Koleva, Solid-state linear-polarized IR-spectroscopic characterization of L-methionine, *Vibrational Spectroscopy* 44 (2007) 30–35.
- [33] E. Podstawka, Y. Ozaki, L.M. Proniewicz, Part I: surface-enhanced Raman spectroscopy investigation of amino acids and their homodipeptides adsorbed on colloidal silver, *Applied Spectroscopy* 58 (2004) 570–580.
- [34] X. Cao, G. Fischer, Conformational and infrared spectral studies of L-methionine and its N-deuterated isotopomer as isolated zwitterions, *Journal of Physical Chemistry A* 106 (2002) 41–50.
- [35] K. Yamamoto, Md. Humayun Kabir, K. Tominaga, Terahertz time-domain spectroscopy of sulfur-containing biomolecules, *Journal of the Optical Society of America B* 22 (2005) 2417–2426.
- [36] A. Grunenber, D. Bougeard, THE observed and calculated vibrational-spectra of dl-methionine in the study of the solid-state phase-transition, *Berichte der Bunsen-Gesellschaft für Physikalische Chemie* 90 (1986) 485–492.
- [37] C. Murli, S. Thomas, S. Venkateswaran, S.M. Sharma, Raman spectroscopic investigation of α-glycine at different temperature, *Physica B: Condensed Matter* 364 (2005) 233–238.
- [38] J.A. Lima Jr., P.T.C. Freire, R.J.C. Lima, A.J.D. Moreno, J. Mendes Filho, F.E.A. Melo, Raman scattering of L-valine crystals, *Journal of Raman Spectroscopy* 36 (2005) 1076–1081.

- [39] A. Trivella, T. Gaillard, R.H. Stote, P. Hellwig, Far infrared spectra of solid state aliphatic amino acids in different protonation states, *Journal of Chemical Physics* 132 (2010) 115105.
- [40] H.D. Middendorf, Biophysical applications of quasi-elastic and inelastic neutron scattering, *Annual Review of Biophysics and Bioengineering* 13 (1984) 425–451.
- [41] G.J. Kearley, A review of the analysis of molecular vibrations using INS, *Nuclear Instruments and Methods A* 53 (1995) 354.
- [42] Jmol, An Open-Source Java Viewer for Chemical Structures in 3D, <http://www.jmol.org/>.
- [43] A. Grunenberg, D. Bougeard, B. Schrader, DSC-investigations of 22 crystalline neutral aliphatic amino acids in the temperature range 233 to 423 K, *Thermochimica Acta* 77 (1984) 59–66.
- [44] J.O. Hutchens, A.G. Cole, J.W. Stout, Heat capacities and entropies of L-cysteine and L-methionine: the transition of L-methionine near 305.5 K, *Journal of Biological Chemistry* 239 (1964) 591–595.
- [45] A. Heidemann, M. Prager, M. Monkenbusch, Methyl rotation in acetamide – the transition from quantum-mechanical tunneling to classical reorientation studied by inelastic neutron scattering, *Zeitschrift für Physik B: Condensed Matter* 76 (1989) 77–88.
- [46] J.M. de Souza, P.T.C. Freire, D.N. Argyriou, J.A. Stride, M. Barthès, W. Kalceff, H.N. Bordallo, Raman and neutron scattering study of partially deuterated L-alanine: evidence of a solid-solid phase transition, *ChemPhysChem* 10 (2009) 3337–3343.
- [47] H.N. Bordallo, E.V. Boldyreva, J. Fischer, M.M. Koza, T. Seydel, V.S. Minkov, V.A. Drebuschak, A. Kyriakopoulos, Observation of subtle dynamic transitions by a combination of neutron scattering, X-ray diffraction and DSC: a case study of the monoclinic L-cysteine, *Biophysical Chemistry* 148 (2010) 34–41.
- [48] S. Clough, A. Heidemann, A.J. Horsewill, J.D. Lewis, M.N.J. Paley, The rate of thermally activated methyl group rotation in solids, *Journal of Physics C: Solid State Physics* 15 (1982) 2495–2508.
- [49] K.T. Jahnke, W. Müller-Warmuth, M. Bennati, Anomalous proton relaxation, rotational tunnelling and barriers to methyl group rotation in solid acetyl halides, *Solid State Nuclear Magnetic Resonance* 4 (1995) 153–161.
- [50] S. Szymanski, Nuclear magnetic resonance line shapes of methyl-like quantum rotors in low-temperature solids, *Journal of Chemical Physics* 111 (1999) 288–299.
- [51] T. Ratajczyk, S. Szymanski, Theory of damped quantum rotation in NMR spectra. I. Fundamental aspects, *Journal of Chemical Physics* 123 (2005) 204509.
- [52] H.-H. Limbach, S. Ulrich, S. Gründemann, G. Buntkowsky, S. Sabo-Etienne, B. Chaudret, G.J. Kubas, J. Eckert, NMR and INS line shapes of transition metal hydrides in the presence of coherent and incoherent dihydrogen exchange, *Journal of the American Chemical Society* 120 (1998) 7929.